

# Cyclic Voltammetry and Electrocatalysis of the Blue Copper Oxidase *Polyporus versicolor* Laccase

Marianne H. Thuesen,<sup>a</sup> Ole Farver,<sup>b</sup> Bengt Reinhammar<sup>c</sup> and Jens Ulstrup<sup>a,\*</sup>

<sup>a</sup>Department of Chemistry, Technical University of Denmark, DK-2800 Lyngby, Denmark, <sup>b</sup>Institute of General Chemistry, Royal Danish School of Pharmacy, DK-2100, Copenhagen, Denmark and <sup>c</sup>Department of Biochemistry and Biophysics, University of Göteborg and Chalmers Institute of Technology, S-402 20 Göteborg, Sweden

## Dedicated to Professor Lennart Ebersson on the occasion of his 65th birthday

Thuesen, M. H., Farver, O., Reinhammar, B. and Ulstrup, J., 1998. Cyclic Voltammetry and Electrocatalysis of the Blue Copper Oxidase *Polyporus versicolor* Laccase. – Acta Chem. Scand. 52: 555–562. © Acta Chemica Scandinavica 1998.

Cyclic voltammetric cathodic and anodic peaks of monolayers of the blue four-copper oxidase *Polyporus versicolor* laccase at edge-plane pyrolytic graphite electrodes under anaerobic conditions have been observed at low ( $\leq 1 \text{ mV s}^{-1}$ ) scan rates. The midpoint potential is  $\approx 790 \text{ mV}$  (vs. NHE) in accordance with the reduction potential in homogeneous solution. The peak separation is 210 mV and the halfwidth about 180 mV. The peak areas correspond approximately to four-electron transfer. This implies that intramolecular electron transfer between the type 1 and the type 2 or type 3 centres combined with interfacial electron transfer at the type 1 or the type 2 and type 3 centre must be part of the mechanism.

Electrocatalytic dioxygen reduction at edge-plane pyrolytic graphite covered with a monolayer of laccase is almost reversible in the cyclic voltammetric and rotating disk modes. The apparent halfwave potential is 750 mV. The limiting current variation with dioxygen concentration follows electrochemical Michaelis–Menten kinetics with insignificant mass transport limitations. The steady-state rate-determining step follows a bell-shaped pH-profile. This step could be either one of the steps of intramolecular electron transfer between the type 1 and type 2/3 centres, or product release. The former gives an average rate constant of  $40 \text{ s}^{-1}$ , the latter  $10\text{--}20 \text{ s}^{-1}$  or about  $10^4 \text{ M}^{-1} \text{ s}^{-1}$  for the maximum second-order rate constant. This accords with values for laccase turnover in homogeneous solution.

Electrochemistry of metalloenzymes holds interesting fundamental and technological perspectives. The former are related to the molecular mechanisms of multi-centre redox proteins, and to electrochemical control of enzyme processes and the two-dimensional protein organization on the electrode surface. Important technological perspectives are related, for example to substrate specificity of immobilized enzymes, and to analytical substrate detection.

Characterizations of multi-centre redox proteins at metallic surfaces are, however, fraught with both principal and practical problems. This contrasts with the often straightforward electrochemical reversibility patterns of small single-metal redox proteins.<sup>1,2</sup> Practical difficulties are the fragile nature of immobilized enzymes, inhomogeneous adsorption, and large, capacitative or

other background currents. Principal problems are the composite nature of multi-electron transfer reactions and the large number of microscopic rate constants and reduction potentials. These can be further complicated by chemical bond reorganization. We have shown recently that *two-centre* proteins are interesting intermediates in the latter respect.<sup>3,4</sup> The electron transfer (ET) behaviour here is still composite and incorporates fundamental cooperativity elements but the overall pattern is simple enough that molecular resolution is within reach.

In this report we address cyclic voltammetry of the four-centre fungal copper oxidase laccase from *Polyporus versicolor*. The catalytic processes of this enzyme class involve the four-electron reduction of molecular dioxygen,<sup>5–8</sup> eqn. (1). We provide new voltammetric data and address perspectives of molecular mechanisms of direct laccase electrochemistry and enzyme electro-

\* To whom correspondence should be addressed.

catalysis of dioxygen reduction. Elements of the molecular electrochemical ET mechanisms are interfacial ET, long-range intramolecular ET between the type 1 (T1) and type 2 (T2) or type 3 (T3) centres, dioxygen reduction and, interestingly and by analogy with ascorbate oxidase, dissociative ET to the T3 centre. These steps can be addressed but the number of reaction steps in the overall, cooperative four-electron processes is far too large for the mechanistic detail accessible in one- and two-centre protein ET patterns.



Kinetic,<sup>9–20</sup> spectroscopic,<sup>21–23</sup> and electrochemical properties<sup>24–33</sup> of the laccases have been investigated. Laccase was the first blue copper oxidase to be investigated in detail.<sup>21</sup> Key questions relate to suggested interactions between the T2 and T3 centres, long-range electronic and conformational interactions between the distant and structurally distinct T1 and T2 or T3 centres, and to protein intermediates in different redox states. T2 and T3 centres are close but these two laccase centres otherwise appear to behave as independent sites in oxidative and reductive titrations.<sup>21</sup> It is also a common notion that T1Cu<sup>II</sup> is a primary electron uptake site while the spatially widely separate T3 centre is the site of the four-electron O<sub>2</sub>-reduction. The three metal centres must therefore be electronically and conformationally linked through the protein. No three-dimensional laccase structures are available, and this functional element has frequently been referred to the structurally characterized, closely homologous ascorbate oxidase in which a 1.22 nm ET channel is indeed conspicuous.<sup>34,35</sup> In laccases, T1Cu<sup>II</sup> reduction, however, also triggers T2Cu<sup>II</sup> reduction by *substrate*. O<sub>2</sub>-reduction at the T3 centre could thus be induced by cooperative intramolecular ET from both the T1 and T2 centres. Most laccase substrates and products are separated by two redox equivalents. All evidence is, however, that reduction of fully oxidized laccase (blue copper oxidases) and enzymatic function proceed by single-ET sequences and radical intermediate formation.<sup>21,36</sup>

The following other specific observations are important: (1) *Rhus* and *P. versicolor* laccase activity proceeds by broadly similar mechanisms<sup>9,14</sup> the pH-dependence of which is prominent. Deprotonation of a T2-coordinated water molecule with parallel attenuation of the enzyme activity is thus a particular feature. The reported pK<sub>a</sub> value of this process is, interestingly rather different for *Rhus* and *P. versicolor* laccase, being about 7.5 and 3.5, respectively [cf. point (3) below]. Also, O<sub>2</sub>-binding during enzyme turnover seems to trigger conformational changes which strongly enhance the ET turnover rates of the copper centres.<sup>9,14,37,38</sup> Such patterns apply to ascorbate oxidase.<sup>19,39</sup> (2) A distinct optically and EPR-detectable intermediate accumulates during steady-state turnover with ascorbate and hydroquinone and excess dioxygen (*Rhus* laccase<sup>10,14</sup>). A likely composition is T1Cu<sup>II</sup>T2Cu<sup>II</sup>T3Cu<sup>II</sup>O<sup>-</sup>. The O<sup>-</sup> radical has the same

spectroscopic properties in native and T2-depleted laccase, which suggests that it is bound to the T3 centre.<sup>36</sup> (3) In addition to the pH-dependent features in point (1) there is a characteristic, bell-shaped pH-profile for the catalytic activity of *Rhus* laccase, with a maximum at pH ≈ 7.5–8, indicative of several protonation equilibria in the different stages of catalytic activity.<sup>17</sup> The activity of *P. versicolor* laccase towards the non-phenolic substrate 1,2,4,5-tetramethylbenzene is, interestingly, highest at much lower pH (≈ 2).<sup>40</sup>

The observations suggest a coarse catalytic scenario which extends to features of laccase electrocatalysis. Intramolecular single-ET prior to O<sub>2</sub>-binding is slow. O<sub>2</sub>-binding to T3 induces a conformational change. This leads to two fast ET steps from T1 and T2 to T3 and liberation of a water molecule, accompanied by fast but kinetically indistinguishable two-proton transfer.<sup>18</sup> This stage is followed by a third ET step leading to bound O<sup>-</sup> formation. The latter is converted into the second water molecule by intramolecular ET and two-proton transfer in a following slow phase. Laccase thus displays a case for cooperative ET where individual ET rates depend strongly on the oxidation states of the copper centres and the number of electrons transferred.

Anaerobic laccase voltammetry under specified conditions is sparse. A *Polyporus versicolor* laccase voltammetric peak at edge-plane pyrolytic graphite at 0.4 V (vs. SSCE) in the presence of 2,9-dimethylphenanthroline (DMP) has been reported.<sup>27</sup> This potential is, however, close to that of Cu<sup>II</sup>-DMP complexes<sup>46</sup> and could be caused by DMP-laccase interaction. Reversible anaerobic laccase voltammetry has also been claimed but with no details as to electrode preparation or enzyme.<sup>29</sup> Other laccases appear to be electrochemically inactive. In comparison, ceruloplasmin exhibits unpromoted voltammetry at graphite.<sup>33</sup> Ascorbate oxidase, being inactive at graphite is reported to show promoted voltammetry at gold surfaces,<sup>41</sup> but specific chemical interaction between the enzyme and the promoter was not reported to have been addressed.

There are a number of studies of surface-immobilized laccase catalysis of electrochemical O<sub>2</sub>-reduction. Tarasevich, Bogdanovskaya and their associates investigated laccase-mediated O<sub>2</sub>-electroreduction using different carbonaceous electrode materials.<sup>24,25,31–33</sup> Reversibility conditions could be mapped in some detail. They also put forward suggestions as to the sequence of electron and proton transfer events based on features in the current-voltage relationships. Cyclic and rotating disk voltammetry for *Polyporus versicolor* laccase electrocatalysis of O<sub>2</sub>-reduction at edge-plane pyrolytic graphite have also been investigated.<sup>27</sup> Mass transport could be deconvoluted and a functional pH-optimum at 2.8–3.8 identified. *Coriolus hirsitus* (fungal) and *Rhus* (tree) laccase are electrochemically inactive under anaerobic conditions but active towards O<sub>2</sub>-reduction at graphite electrodes.<sup>33</sup> These enzymes also exhibit characteristic functional pH-optima. This is in interesting contrast with

ceruplasmin and tyrosinase, which show the inverse behaviour, and accord with views on mechanistic differences of these enzymes in homogeneous solution. The laccases thus appear to exploit a stepwise mechanism, whereas ceruloplasmin and tyrosinase catalysis proceeds via ternary complex formation. Other observations of laccase electrocatalysis are reported in Refs. 29 and 32. Fungal laccases have finally been incorporated into enzyme sensor systems for detection of phenolic compounds in electrochemical and flow injection configurations.<sup>42,43</sup>

We report here new, four-electron anaerobic cyclic voltammetry and electrocatalytic dioxygen reduction of *Polyporus versicolor* laccase at edge-plane pyrolytic graphite. Promoters showed little effect. Anaerobic laccase reduction and oxidation give broad peaks with a midpoint potential around 790 mV (NHE). The electrocatalytic mode follows electrochemical Michaelis–Menten kinetics, with a pH-optimum at  $\text{pH} \approx 3.3$ . The data provide rate constants for the catalytic turnover which can be compared with *Polyporus versicolor* laccase activity in homogeneous solution.

## Experimental

Millipore water and analytical grade reagents were used. The purity of argon (99.999%) was further controlled by Chrompack column purification. *Polyporus versicolor* laccase was isolated as described.<sup>44</sup> The enzyme was purified on DEAE Sephadex A50. Fluoride was removed by diafiltration (Amicon model 8200, YM3 membranes) to 5 mM ascorbate, 0.1 M phosphate, pH 6.0, followed by diafiltration to 0.1 M phosphate, pH 6.0. The  $A_{280}/A_{610}$  absorbance ratio was 17–20 and concentrations determined from the absorbance at 610 nm ( $\epsilon = 4.900 \text{ M}^{-1} \text{ cm}^{-1}$ ).<sup>44,45</sup>

Pyrolytic graphite (PG) electrodes were machined from 6 mm PG cylinders (Union Carbide) and mounted on brass cylinders with silver-loaded two-component epoxy (RS components), the edge plane facing the solution. The brass–PG cylinder was cemented into Teflon holders with two-component epoxy (EpoxyLite 3151). The electrode surface was polished with 1200, 2400 and 4000 grit silicon carbide paper (DragonFly), and  $0.1 \mu\text{m Al}_2\text{O}_3$  water suspension, rinsed, and treated ultrasonically.

Electrochemical measurements were recorded by means of an Eco Chemie Autolab potentiostat equipped with an ECD low current module, and controlled by the general purpose Electrochemical System version 3.2 Eco Chemie software. The cell was a three-electrode, two-compartment all-glass cell with the working and reference chamber separated by a Luggin capillary. The reference electrode was a Ag/AgCl/3 M KCl electrode (Metrohm, 210 mV vs. SCE) fitted with a glass salt bridge (Metrohm) containing 0.1 M KCl. All potentials are referred to the SHE. The counter electrode was a semi-cylindrical platinum gauze positioned opposite to the

Luggin capillary tip. An EG&G Princeton Applied Research model 636 rotating disk set-up was used for the rotating disk electrode experiments.

The cell held an additional entrance for positioning a  $p\text{O}_2$ -sensor (Clark type  $p\text{O}_2$ -sensor) connected to an OM-4 oxygen meter (Microelectrodes). The dioxygen concentration in the solution was controlled by bubbling mixtures of water-saturated dioxygen and argon through the electrode chamber. The  $\text{O}_2/\text{Ar}$  ratio was regulated by two mass flowmeters (Brooks, model 5850TR) and a microprocessor control and readout unit (Brooks, model 0152).

*P. versicolor* laccase (typically 5  $\mu\text{l}$ , 0.5  $\mu\text{M}$  or approximately one monolayer) was applied to a freshly polished PG edge plane electrode surface. The enzyme-covered electrode was dried ( $\approx 30$  min) and electrochemical experiments then initiated. The solution contained no free enzyme. The temperature was 21–23 °C. Solutions were 20 mM acetate or 30 mM citrate buffers, ionic strength  $I = 0.1 \text{ M}$  (sodium perchlorate). Solutions for the chronoamperometric experiments were 30 mM citrate,  $I = 0.1 \text{ M}$  ( $\text{NaClO}_4$ ). The electrodes were here pre-treated under turnover conditions (360 mV,  $\text{O}_2$ -saturated solution) for 25 min prior to the experiments.

## Results

*Cyclic and rotating disk voltammetry.* Fig. 1 shows cyclic voltammograms of pre-adsorbed *P. versicolor* laccase on PGE electrodes in an  $\text{O}_2$ -free atmosphere,  $\text{pH} = 3.3$ , which is both the optimum for catalytic activity and close to the isoelectric point. The voltammograms are representative of low scan rates (shown for  $1 \text{ mV s}^{-1}$ ). Voltammetric peaks clearly appear. The midpoint potential is 790 mV, which is close to the reduction potential in homogeneous solution.<sup>45</sup> The peak separation is 210 mV and full width at half height  $\approx 180$  mV. This is indicative of distinct but notably irreversible anaerobic electrochemical activity. These currents are thus several orders of magnitude larger than catalytic currents caused by residual dioxygen. In addition, both cathodic and anodic signals were systematically observed. The total charge corresponding to the area under the current–time relationship of the background-corrected voltammogram (most accurate for the cathodic peak) is, furthermore  $\approx 1.1 \times 10^{-6} \text{ C}$ . This is close to complete four-electron turnover of the 2.5 pmol of enzyme deposited on the surface.

The peaks are blurred by increasing background at scan rates higher than  $1 \text{ mV s}^{-1}$ . The promoter polymyxin had no effect. Addition of 2,9-dimethylphenanthroline generated new redox signals with a midpoint potential of 660 mV (cf. Ref. 27). A very similar signal appeared when  $\text{CuSO}_4$  was titrated into DMP-containing electrolyte solution in the absence of enzyme. The 660 mV signal is therefore likely to be caused by  $\text{Cu}^{\text{II}}$  complex formation with DMP. Mono- and bis-

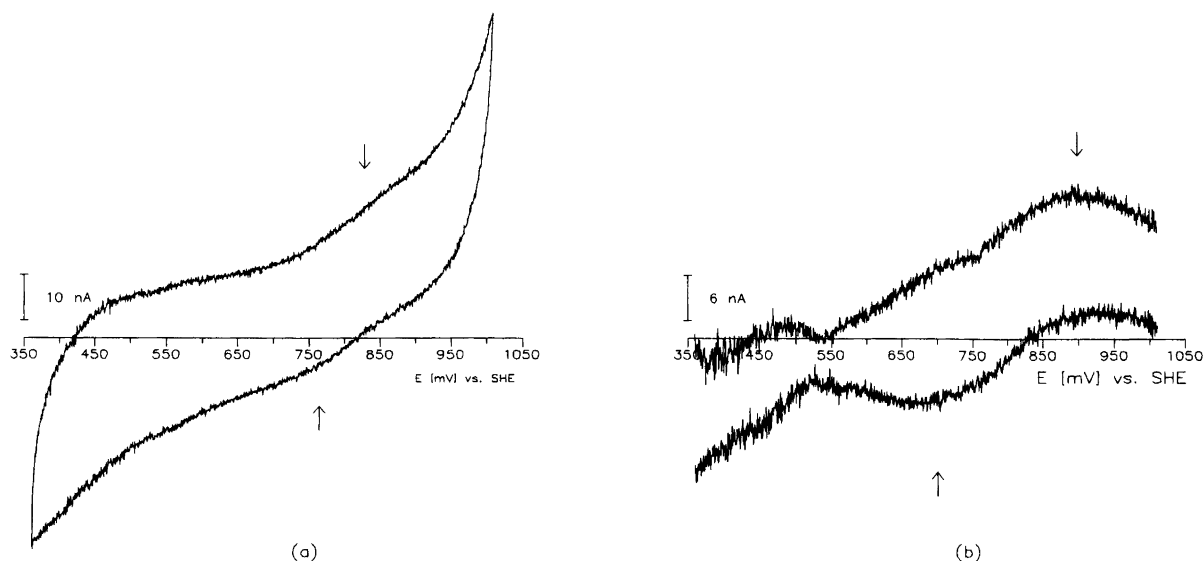


Fig. 1. (a) Cyclic voltammety (second scan) of 2.5 pmol *P. versicolor* laccase adsorbed onto a PGE electrode. Anaerobic conditions. 30 mM citrate, pH 3.31. Ionic strength 0.1 M ( $\text{NaClO}_4$ ). Scan rate  $1 \text{ mV s}^{-1}$ . (b) The background-corrected signal.

DMP complexes of  $\text{Cu}^{\text{II}}$  have also been shown to catalyse the electrochemical reduction of dioxygen.<sup>46</sup>

Catalytic currents appeared in the presence of dioxygen (Fig. 2). The signal decreased over the first 30 min and then stabilized. The character of the wave and the current plateau reflect the electrocatalytic function of the immobilized enzyme (cf. Ref. 27). The potential where the current is 50% of the plateau value is  $\approx 750 \text{ mV}$ . This is close to the reversible potential of *P. versicolor* laccase and to the midpoint potential in Fig. 1 but lower than the potential for reversible dioxygen reduction to water ( $\approx 1.0 \text{ V}$ ). The Faradaic current is almost independent of the scan rate up to  $30 \text{ mV s}^{-1}$ . In the rotating disk mode it is also independent of the speed of rotation in

the range 0–1000 rpm. A 10% current increase from 100–900 rpm has previously been noted.<sup>27</sup> The small effect shows that the catalytic turnover is slow enough that virtually no dioxygen depletion occurs close to the electrode.

#### Chronoamperometry and electrocatalytic enzyme kinetics.

The catalytic current was recorded at the sensing potential of 360 mV for a range of dioxygen concentrations and the pH range 2.50–5.10. Increasing amounts of dioxygen were introduced in a step-like procedure and the current increase recorded. This was followed by successive concentration decrease after the maximum concentration ( $\approx 1.2 \text{ mM}$ ) corresponding to saturation of the solution. Laccase-covered electrodes always responded immediately to the dioxygen level (Fig. 3). The current ( $i$ ) dependence on  $[\text{O}_2]$  is shown in Fig. 4.

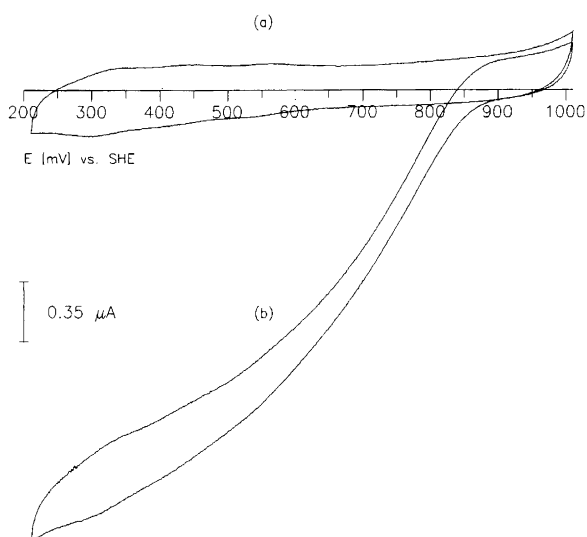


Fig. 2. Cyclic voltammety (second scan) of  $\approx 17 \text{ pmol}$  *P. versicolor* laccase on a PGE electrode. 20 mM acetate, pH 3.82. Ionic strength 0.1 M ( $\text{NaClO}_4$ ). Scan rate  $10 \text{ mV s}^{-1}$ : (a) in the absence of dioxygen; (b) 1.2 mM dioxygen.

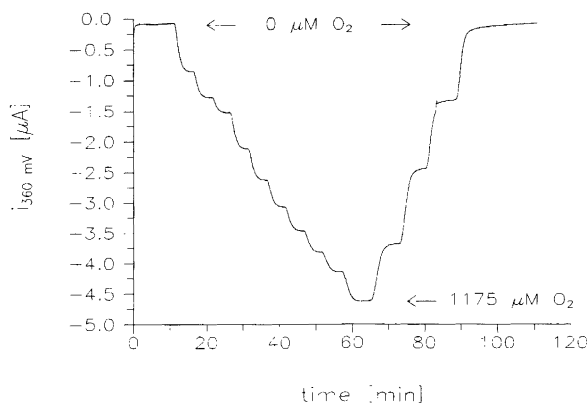


Fig. 3. Chronoamperometry of 2.5 pmol *P. versicolor* laccase on a PGE electrode. Gradual increase and subsequent decrease of  $[\text{O}_2]$  ( $0 \rightarrow 1.175 \text{ mM} \rightarrow 0$ ). 30 mM citrate, pH 3.31. Ionic strength 0.1 M ( $\text{NaClO}_4$ ). Recording potential 360 mV vs. (SHE).

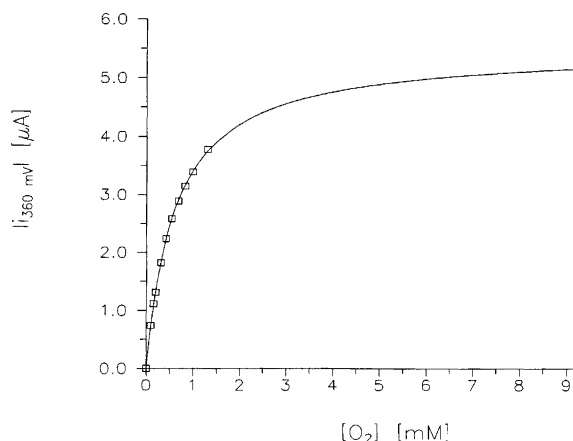


Fig. 4. Electrochemical Michaelis–Menten plot of background-corrected chrono-amperometric data for electrocatalytic  $\text{O}_2$ -reduction by  $\approx 2.5$  pmol *P. versicolor* laccase adsorbed onto a PGE electrode. Conditions as in Fig. 3. The line is based on Michaelis–Menten fit.  $K_{\text{M,obs}} = 612 \mu\text{M}$ ,  $i_{\text{max,obs}} = 5.50 \mu\text{A}$ .

$i$  approaches a limiting value  $i_{\text{max}}$ , at high  $[\text{O}_2]$ . The correlation is well represented by the electrochemical Michaelis–Menten form, eqn. (2), where  $K_{\text{M,obs}}$  is the apparent Michaelis–Menten constant.  $i_{\text{max}}$  can be related to the Michaelis–Menten rate constant,  $k_{\text{cat,obs}}$ , and the enzyme coverage  $\Gamma_{\text{laccase}}$ , according to eqn. (3),

$$i = \frac{i_{\text{max}}[\text{O}_2]}{K_{\text{M,obs}} + [\text{O}_2]} \quad (2)$$

$$i_{\text{max}} = nFk_{\text{cat,obs}}\Gamma_{\text{laccase}}A \quad (3)$$

where  $n$  is the number of electrons transferred,  $F$  the Faraday number, and  $A$  the electrode area.  $i_{\text{max}}/nF$  is the electrochemical analogue of the maximum turnover number,  $V_{\text{max}}$ , of enzyme kinetics in homogeneous solution.

The chronoamperometric data were fitted to eqns. (2) and (3). The pH-profiles of  $k_{\text{cat,obs}}$  and  $K_{\text{M,obs}}$ , and of the second-order rate constant  $k_{\text{cat,obs}}/K_{\text{M,obs}}$  are shown in Fig. 5, and follow a bell-shape (cf. Refs. 17 and 27). Full 2.5 pmol monolayer function was assumed in the conversion of  $i_{\text{max}}$  into  $k_{\text{cat,obs}}$ . The error bars refer to the data analysis and not to  $\Gamma_{\text{laccase}}$ .

## Discussion

The most interesting observations of the present investigation are anaerobic *P. versicolor* laccase voltammetry and the electrocatalytic Michaelis–Menten kinetics.

*Anaerobic electrochemical laccase behaviour.* Unpromoted anaerobic voltammetry of adsorbed laccase on PGE in both cathodic and anodic scans was obtained (Fig. 1). The maximum currents are in the 5–10 nA range which is far higher than catalytic currents caused by residual dioxygen reduction. The midpoint potential of 790 mV (vs. SHE) accords with potentiometrically

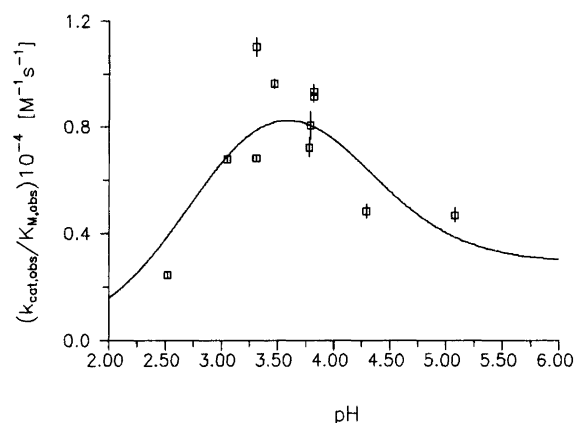
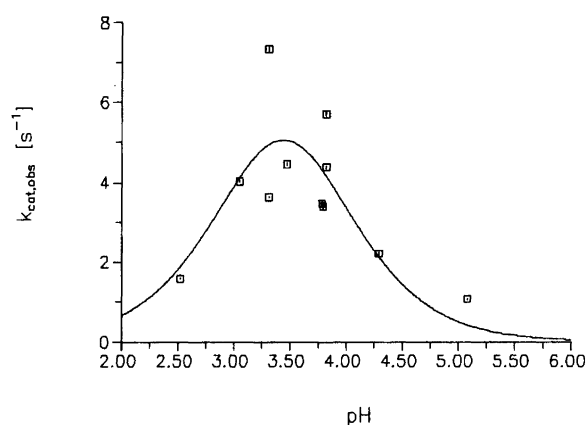
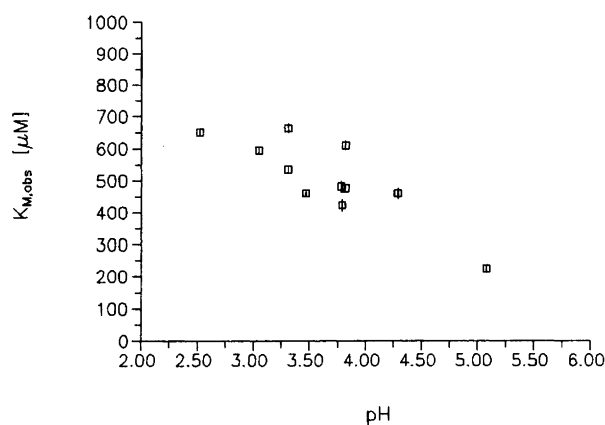


Fig. 5. pH-dependence of the apparent kinetic parameters from the data in Figs. 3 and 4: (a)  $K_{\text{M,obs}}$  ( $\mu\text{M}$ ); (b)  $k_{\text{cat,obs}}$  ( $\text{s}^{-1}$ ); (c)  $k_{\text{cat,obs}}/K_{\text{M,obs}}$  ( $\text{M}^{-1} \text{s}^{-1}$ ).

determined values for T1 and T3.<sup>45</sup> The estimation of the total charge turnover is crude but still testifies to a flow of *four* electrons per molecule. This is interesting and indicates that full electrochemical activity of all the copper atoms of immobilized laccase A is maintained in the non-catalytic mode.

The wide (210 mV) separation of the broad (180 mV) cathodic and anodic peaks points to ‘irreversible’ behavi-

our. Conceivable physical origins of this are: (a) Direct, slow electron transfer (ET) to both T1 and T2 or T3; (b) inhomogeneous adsorption patterns, incorporating physical interaction between laccase molecules on the surface; (c) interfacial ET coupled to intramolecular ET between T1 and T2 or T3. This would in fact be a condition that approximately *four* electrons be turned over. In addition intramolecular ET holds at least *two* physical implications:

(i) Slow intramolecular ET would affect the voltammetric shape. Slow ET would be rooted in the dissociative ET feature at the T3 centre. This would add reorganization Gibbs free energy along the low-frequency stretching mode in the reduced T3 state where the chemical bond between the copper atoms is essentially broken. Instead of the broadly used quadratic activation Gibbs free energy form,<sup>47</sup> eqn. (4), the following different form [eqn. (5)] emerges.

$$G^\ddagger = (E_R + \Delta G^\circ)^2/4E_R \quad (4)$$

$$G^\ddagger = (E_R + E_R^{\text{CuCu}} + \Delta G^\circ)^2/4E_R \quad (5)$$

$E_R$  is the reorganization Gibbs free energy of all the other, linear molecular and solvent modes in the individual microscopic ET steps and  $\Delta G^\circ$  the driving force.  $E_R^{\text{CuCu}}$  is the reorganization energy along the Cu–Cu stretching mode in the T3 centre after this bond is broken. Eqn. (5) was first introduced in dissociative ligand substitution,<sup>48,49</sup> and later incorporated into the formalism of dissociative *electron transfer*.<sup>50–52</sup>

(ii) The voltammograms incorporate a *distribution* of interfacial and intramolecular single-ET steps, each inducing shifts in microscopic reduction potentials and rate constants. The number of microscopic parameters is large, but resolution can be approached by methods for composite metalloprotein electrochemical analysis.<sup>4</sup>

**Laccase A catalyzed electrochemical dioxygen reduction: enzyme kinetics.** The observation of electrocatalytic dioxygen reduction (Fig. 2) accords with previous work.<sup>27</sup> Other investigations are available for cytochrome *c* peroxidase,<sup>53</sup> glucose oxidase,<sup>54,55</sup> fumarate reductase<sup>56</sup> horseradish peroxidase,<sup>57</sup> and *Rhus* laccase.<sup>33</sup> The following factors affect the turnover rate in immobilized mono- and sub-monolayer enzyme electrocatalysis: (a) Transport of substrate to the surface. The current independence of both scan rate and rotation speed, however, indicates that transport limitations are of minor importance. (b) Reaction between immobilized enzyme and substrate. This overall composite step is incorporated into the steady-state electrochemical rate constants. The  $\text{O}_2$ -concentration dependence points to the importance of this step. (c) Intramolecular ET: this is likely to be important (cf. above). Cooperativity and conformational changes induced by dioxygen binding point to a composite nature of this step and to rate constants different from those in anaerobic electrochemistry. (d) Product dissociation: this step also cannot *a priori* be excluded as rate-determining. (e) Interfacial electrochemical ET: this

must be important at the higher potentials. At the low sensing potential used to record the Michaelis–Menten kinetics the electrocatalytic turnover is, however, determined by the other steps listed.

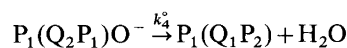
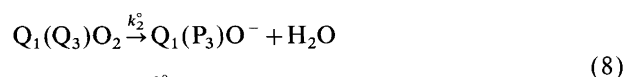
**Features of mechanism.** As for anaerobic laccase voltammetry, resolution of the mechanism could be approached by combination with numerical simulation of the voltammograms. The number of microscopic parameters in the four-ET catalysed dioxygen reduction is, however, prohibitive. A suitable first step could focus on the steady-state feature of the voltammogram in Fig. 2. This still requires a minimum of 25 forward and reverse single-ET steps. The steady-state current reproduces eqn. (2),  $i_{\text{max}}$  and  $K_{\text{M,obs}}$  incorporating the manifold of microscopic rate constants. By associating rate limitation with particular steps, rate constants of the latter can, however, be disentangled to some extent. For example:

(a) If intramolecular ET is rate determining, then eqn. (6) holds.  $i$  refers to four consecutive intramolecular single-ET steps. These cannot be separated. The ‘average’ value is  $(k_{ii})_{\text{av}} \approx 40 \text{ s}^{-1}$  during steady-state turnover. In comparison, values in excess of  $100 \text{ s}^{-1}$  for homogeneous solution have been reported.<sup>39,58</sup>

$$k_{\text{cat,obs}}^{-1} = \sum_i k_{ii}^{-1} \quad i = 1, 2, 3, 4 \quad (6)$$

(b) When product dissociation is rate determining, say at high  $[\text{O}_2] \gg K_{\text{M,obs}}$ , then eqn. (7) holds, where  $k_2^\circ$  and  $k_4^\circ$  refer to steps (8) and (9). P and Q are the oxidized and reduced form, respectively of the copper atoms. P and Q outside the bracket represent T1, inside the bracket the T2 and T3 centres. The subscript indicates the number of copper atoms in the particular oxidation state.

$$k_{\text{cat,obs}}^{-1} = (k_2^\circ)^{-1} + (k_4^\circ)^{-1} \quad (7)$$



The values of  $k_{\text{cat,obs}}$  are shown in Fig. 5.  $k_{\text{cat,obs}}/K_{\text{M,obs}}$  in the two limits is given respectively, by eqn. (9), where  $k_1^\circ$  is the rate constant of step (10), and  $K_{11}$  the equilibrium constant for the intramolecular process (11).

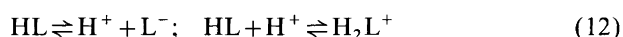
$$k_{\text{cat,obs}}/K_{\text{M,obs}} = k_1^\circ/(1 + K_{11}) \quad \text{and} \quad (9)$$

$$k_{\text{cat,obs}}/K_{\text{M,obs}} = k_1^\circ$$



The pH-profile suggests that at least two ionizing groups are engaged in the rate-limiting step (Fig. 5).  $k_{\text{cat,obs}}/K_{\text{M,obs}}$  and  $k_{\text{cat,obs}}$  reflect, moreover the behaviour of the free enzyme and the enzyme–substrate complex, respectively. Provided that the same rate-determining step is retained over the whole pH-range, the data in Fig. 5 can be fitted to the simple equilibrium scheme (12),

where HL is the laccase form at the pH-maximum. In principle *all* the interfacial and intramolecular ET steps would follow such a pattern. The best fits of eqn. (12), and a single steady-state rate-determining step are shown in Fig. 5. The parameters are given in Table 1. The following observations are apparent: (a) There is a maximum in the kinetic pH-profiles, in both cases at *ca.* pH 3.3, the halfwidth being about one pH-unit. This follows a previous observation<sup>27</sup> except that the steady-state kinetics are now resolved and the profiles are notably sharper. (b) The apparent  $pK_A$ -values are closely spaced. In view of the scatter, the different values for the two profiles is hardly significant. (c) The turnover is dominated by the mono-protonated laccase form even though the  $k_{\text{cat,obs}}/K_{\text{M,obs}}$ -profile gives a finite rate constant of the deprotonated form. (d) If intramolecular ET is rate-determining, cooperativity disregarded, and all intramolecular rate constants coincide,  $k_{nn} \approx 40 \text{ s}^{-1}$  ( $n = 1, 2, 3, 4$ ) for the mono-protonated form. If the reduction potential difference between the T1 and T2/3 centres is 3 mV, then  $k_1^\circ \approx 2 \times 10^{-4} \text{ M}^{-1} \text{ s}^{-1}$  [eqn. (10)]. If product release is rate-determining and the two rate constants in eqn. (7) are of the same order, then  $k_2^\circ \approx k_4^\circ \approx 20 \text{ s}^{-1}$  and  $k_1^\circ \approx 10^4 \text{ M}^{-1} \text{ s}^{-1}$  for monoprotated laccase. These values also accord with a previous report of  $1.5 \times 10^4 \text{ M}^{-1} \text{ s}^{-1}$  for immobilized *Polyporus versicolor* laccase.<sup>27</sup>



In conclusion we have shown that immobilized *Polyporus versicolor* laccase can exhibit anaerobic four-electron cyclic voltammetry. The midpoint potential accords with the known reduction potentials of the copper centres. Interfacial ET involving the T1 centre combined with intramolecular ET is likely but cannot be distinguished from parallel interfacial ET at different centres. Catalytic voltammograms in the presence of dioxygen have been obtained and shown to follow electrochemical Michaelis-Menten behaviour. The voltammograms hold information about the molecular mechanisms. Subject to the notion of a rate-determining step, alternative values of the rate constants for intramolecular ET or product release in the catalytic process could be estimated by a simple, steady-state approach. These are  $\approx 40 \text{ s}^{-1}$  and  $\approx 20 \text{ s}^{-1}$ , respectively, and in the

**Table 1.** Kinetic parameters from the pH-profiles in Fig. 5.  $k_1$ ,  $k_2$  and  $k_3$  are the rate constants of  $\text{L}^-$ , HL and  $\text{H}_2\text{L}^+$ , respectively, in eqn. (12).  $K_1$  and  $K_2$  are the acid dissociation constants of HL and  $\text{H}_2\text{L}^+$ , respectively.

Parameter	$k_{\text{cat,obs}}/\text{s}^{-1}$	$k_{\text{cat,obs}}(K_{\text{M,obs}})^{-1}/\text{M}^{-1} \text{ s}^{-1}$
$k_1$	0	$3 \times 10^3$
$k_2$	10	$10^4$
$k_3$	0	0
$pK_1$	3.7	4.2
$pK_2$	3.2	2.8

same range as for laccase turnover in homogeneous solution.<sup>39</sup>

**Acknowledgements.** Financial support from The Danish Natural Science and Technical Science Research Councils, The Carlsberg Foundation, The Lundbeck Foundation, Direktør, dr. techn. A.N. Neergaards og Hustrus Foundation, and Novo Nordisk Foundation is acknowledged.

## References

1. Armstrong, F. A. *Struct. Bond.* 72 (1990) 137.
2. Guo, L. H. and Hill, H. A. O. *Adv. Inorg. Chem.* 36 (1991) 341.
3. Conrad, L. S., Karlsson, J.-J. and Ulstrup, J. *Eur. J. Biochem.* 231 (1995) 133.
4. Karlsson, J.-J., Nielsen, M. F., Thuesen, M. H. and Ulstrup, J. *J. Phys. Chem.* 101 (1997) 2430.
5. Farver, O. and Pecht, I. In: Lontie, R., Ed., *Copper Proteins and Copper Enzymes, Vol I*, CRC Press, Boca Raton 1984, p. 183.
6. Morpurgo, L. *Life Chem. Rep.* 5 (1987) 277.
7. Messerschmidt, A. and Huber, R. *Eur. J. Biochem.* 187 (1990) 341.
8. Farver, O. In: Bendall, D. S., Ed., *Protein Electron Transfer*, Bios Scientific, Oxford 1996, p. 161.
9. Andréasson, L.-E. and Reinhammar, B. *Biochim. Biophys. Acta* 445 (1976) 579.
10. Andréasson, L.-E., Brändén, R. and Reinhammar, B. *Biochim. Biophys. Acta* 438 (1976) 370.
11. Aasa, R., Brändén, R., Deinum, J., Malmström, B. G., Reinhammar, B. and Vänngaard, T. *FEBS Lett.* 61 (1976) 115.
12. Brändén, R. and Deinum, J. *Biochim. Biophys. Acta* 524 (1978) 297.
13. Aasa, R., Brändén, R., Deinum, J., Malmström, B. G., Reinhammar, B. and Vänngaard, T. *Biochem. Biophys. Res. Commun.* 70 (1976) 1204.
14. Andréasson, L.-E. and Reinhammar, B. *Biochim. Biophys. Acta* 568 (1979) 145.
15. (a) Holwerda, R. A. and Gray, H. B. *J. Am. Chem. Soc.* 96 (1974) 6008; (b) 97 (1975) 6036.
16. Clemmer, J. D., Gilliland, B. L., Bartsch, R. A. and Holwerda, R. A. *Biochim. Biophys. Acta* 568 (1979) 307.
17. Koudelka, G. B., Hansen, F. B. and Ettinger, M. J. *J. Biol. Chem.* 260 (1985) 15561.
18. Reinhammar, B. *Chem. Scr.* 25 (1985) 172.
19. Farver, O. and Pecht, I. *FASEB J.* 5 (1991) 2554.
20. Tollin, G., Meyer, T. E., Cusanovich, M. A., Curir, P. and Marchesini, A. *Biochim. Biophys. Acta* 1183 (1993) 309.
21. Reinhammar, B. In: Lontie, R., Ed., *Copper Proteins and Copper Enzymes*, CRC Press, Boca Raton 1984, p. 1.
22. Cole, J. L., Avigliano, L., Morpurgo, L. and Solomon, E. I. *J. Am. Chem. Soc.* 113 (1991) 9080.
23. Clark, P. A. and Solomon, E. I. *J. Am. Chem. Soc.* 114 (1992) 1108, and references there.
24. Berezin, I. V., Bogdanovskaya, V. A., Varfolomeev, S. D., Tarasevich, M. R. and Yaropolov, A. I. *Dokl. Akad. Nauk SSSR* 240 (1978) 615.
25. Tarasevich, M. R., Yaropolov, A. I., Bogdanovskaya, V. A. and Varfolomeev, S. D. *Bioelectrochem. Bioenerg.* 6 (1979) 393.
26. Taniguchi, V. T., Malmström, B. G., Anson, F. C. and Gray, H. B. *Proc. Natl. Acad. Sci. USA* 79 (1982) 3387.
27. Lee, C.-W., Gray, H. B., Anson, F. C. and Malmström, B. G. *J. Electroanal. Chem.* 172 (1984) 289.

28. Cenas, N. K., Pocius, A. K. and Kulys, J. J. *Bioelectrochem. Bioenerg.* 12 (1984) 583.
29. Yaropolov, A. I. and Ghindilis, A. L. *Elektrokhimiya* 21 (1985) 982.
30. Tarasevich, M. R., Bogdanovskaya, V. A., Gavrilova, E. F. and Orlov, S. B. *J. Electroanal. Chem.* 206 (1986) 217.
31. Kuznetsov, A. M., Bogdanovskaya, V. A., Tarasevich, M. R. and Gavrilova, E. F. *FEBS Lett.* 215 (1987) 219.
32. Bogdanovskaya, V. A. and Tarasevich, M. R. *Sov. Sci. Rev. B. Chem.* 17 (1992) 1.
33. Yaropolov, A. I., Kharybin, A. N., Emnéus, J., Marko-Varga, G. and Gorton, L. *Bioelectrochem. Bioenerg.* 40 (1996) 49.
34. Messerschmidt, A., Rossi, A., Ladenstein, R., Huber, R., Bolognesi, M., Gatti, G., Marchesini, A., Petruzzelli, R. and Finazzi-Agró, A. *J. Mol. Biol.* 206 (1989) 513.
35. Messerschmidt, A., Luecke, H. and Huber, R. *J. Mol. Biol.* 230 (1993) 997.
36. Reinhammar, B., In: Bertini, I., Drago, R. S. and Luchinat, C., Eds., *The Coordination Chemistry of Metalloenzymes*, Reidel, Dordrecht, 1983, p. 177.
37. Goldberg, M., Farver, O. and Pecht, I. *J. Mol. Biol.* 255 (1980) 7353.
38. Andréasson, L.-E., Malmström, B. G., Strömberg, O. and Beinhammar, B., *Eur. J. Biochem.* 34 (1973) 434.
39. (a) Farver, O. and Pecht, I. *Proc. Natl. Acad. Sci. USA* 89 (1992) 8283; (b) *J. Biol. Chem.* 269 (1994) 22933.
40. Kersten, P. J., Kalyanaraman, B., Hammel, K. E., Reinhammar, B. and Kirk, K. *Biochem. J.* 268 (1990) 475.
41. Sakurai, T. *Chem. Lett.* (1996) 481.
42. Ghindilis, A. L., Gavrilova, V. P. and Yaropolov, A. I. *Biosensors and Bioelectronics* 7 (1992) 127.
43. Wang, J., Lin, Y., Eremenko, A. V., Ghindilis, A. L. and Kurochkin, I. N. *Anal. Lett.* 26 (1993) 197.
44. Fåhræus, G. and Reinhammar, B. *Acta Chem. Scand.* 21 (1967) 2367.
45. Reinhammar, B. R. M. *Biochim. Biophys. Acta* 275 (1972) 245.
46. Lei, Y. and Anson, F. C. *Inorg. Chem.* 33 (1994) 5003.
47. For the origin of this form, see: Hush, N. S. and Ulstrup, J. In: Kornyshev, A. A., Tosi, M. P. and Ulstrup, J., Eds., *Electron and Ion Transfer in Condensed Media*, World Scientific, Singapore, 1997. In press.
48. German, E. D. and Dogonadze, R. R. *J. Res. Inst. Hokkaido Univ.* 20 (1972) 34.
49. German, E. D. and Dogonadze, R. R. *Int. J. Chem. Kinet.* 6 (1974) 457, 467.
50. Ulstrup, J. In: Lund, H., Ed., *Proc. Sandbjerg Meeting on Organic Electrochemistry*, Aarhus University, 1982, p. 1.
51. Savéant, J. *J. Am. Chem. Soc.* 109 (1987) 6788.
52. German, E. D. and Kuznetsov, A. M. *J. Phys. Chem.* 98 (1994) 6120.
53. Scott, D. L. and Bowden, E. *Anal. Chem.* 66 (1994) 1217.
54. Kamin, R. A. and Wilson, G. S. *Anal. Chem.* 52 (1980) 1198.
55. Mell, L. D. and Maloy, J. T. *Anal. Chem.* 47 (1975) 299.
56. Sucheta, A., Cammick, R., Weiner, J. and Armstrong, F. A. *Biochemistry* 32 (1993) 5455.
57. Ruzgas, T., Gorton, L., Emnéus, J. and Marko-Varga, G. *J. Electroanal. Chem.* 391 (1995) 41.
58. Varfolomeev, S. D., Naki, A., Yaropolov, A. I. and Berezin, I. V. *Biokhimiya* 50 (1985) 1203.

Received May 5, 1997.